crystals

MDPI

Review

Physiological Metals Can Induce Conformational Changes in Transthyretin Structure: Neuroprotection or Misfolding Induction?

Lidia Ciccone [1,2,*,†], Nicolò Tonali [3,†], William Shepard [2], Susanna Nencetti [1] and Elisabetta Orlandini [4,5]

[1] Department of Pharmacy, University of Pisa, via Bonanno 6, 56126 Pisa, Italy; susanna.nencetti@unipi.it
[2] Synchrotron SOLEIL, L'Orme des Merisiers, Saint-Aubin, BP 48, 91192 Gif-sur-Yvette, France; william.shepard@synchrotron-soleil.fr
[3] Université Paris-Saclay, CNRS, BioCIS, rue Jean-Baptiste Clément 5, 92290 Châtenay-Malabry, France; nicolo.tonali@universite-paris-saclay.fr
[4] Department of Earth Sciences, University of Pisa, via Santa Maria 53, 56126 Pisa, Italy; elisabetta.orlandini@unipi.it
[5] Research Center "E. Piaggio", University of Pisa, 56122 Pisa, Italy
* Correspondence: lidia.ciccone@unipi.it; Tel.: +39-050229531
† These authors contributed equally to the manuscript.

Abstract: Transthyretin (TTR) is a plasma homotetrameric protein that transports thyroxine and retinol. TTR itself, under pathological conditions, dissociates into partially unfolded monomers that aggregate and form fibrils. Metal ions such as Zn^{2+}, Cu^{2+}, Fe^{2+}, Mn^{2+} and Ca^{2+} play a controversial role in the TTR amyloidogenic pathway. TTR is also present in cerebrospinal fluid (CSF), where it behaves as one of the major Aβ-binding-proteins. The interaction between TTR and Aβ is stronger in the presence of high concentrations of Cu^{2+}. Crystals of TTR, soaked in solutions of physiological metals such as Cu^{2+} and Fe^{2+}, but not Mn^{2+}, Zn^{2+}, Fe^{3+}, Al^{3+}, Ni^{2+}, revealed an unusual conformational change. Here, we investigate the effects that physiological metals have on TTR, in order to understand if metals can induce a specific and active conformation of TTR that guides its Aβ-scavenging role. The capability of certain metals to induce and accelerate its amyloidogenic process is also discussed.

Keywords: transthyretin; neuroprotection; metal ions; altered conformations; amyloidoisis; Aβ scavenger; Zn^{2+}; Cu^{2+}; Fe^{2+}; Ca^{2+}

Citation: Ciccone, L.; Tonali, N.; Shepard, W.; Nencetti, S.; Orlandini, E. Physiological Metals Can Induce Conformational Changes in Transthyretin Structure: Neuroprotection or Misfolding Induction?. *Crystals* **2021**, *11*, 354. https://doi.org/10.3390/cryst11040354

Academic Editor: Pawan Mishra

Received: 25 February 2021
Accepted: 25 March 2021
Published: 29 March 2021

1. Introduction

Human transthyretin (TTR), or prealbumin, is a homotetrameric protein mainly synthesized in the liver and secreted into the serum. However, a small amount of TTR is also produced in the retina and choroid plexuses of the brain [1]. The acronym TTR encloses the principal protein's physiological functions: transporter, thyroxine (T4) and retinol in plasma and in cerebrospinal fluid (CSF). While T4 molecules are directly bound to the TTR binding sites, retinol is transported by TTR through its interaction with retinol-binding protein (RBP), which binds orthogonally to T4 [2].

The TTR structure is characterized by four identical 127 amino acid β-sheet sandwich subunits (A, B, A′ and B′) assembled together in a molecular 222 symmetry, Figure 1a. The two dimers (A-B and A′-B′) are oriented to form a central channel that crosses the entire tetramer where T4 binds, Figure 1b [3]. Each monomer folds into a β-sandwich characterized by two β-sheets that consist of four anti-parallel β-strands, DAGH, and CBEF. One short segment of α-helix and a flexible loop connect the β-strands E and F, Figure 1c. The four β-strands DAGH of the four monomers define the channel's surface of the tetramer, while β-strands CBEF design the external surface.

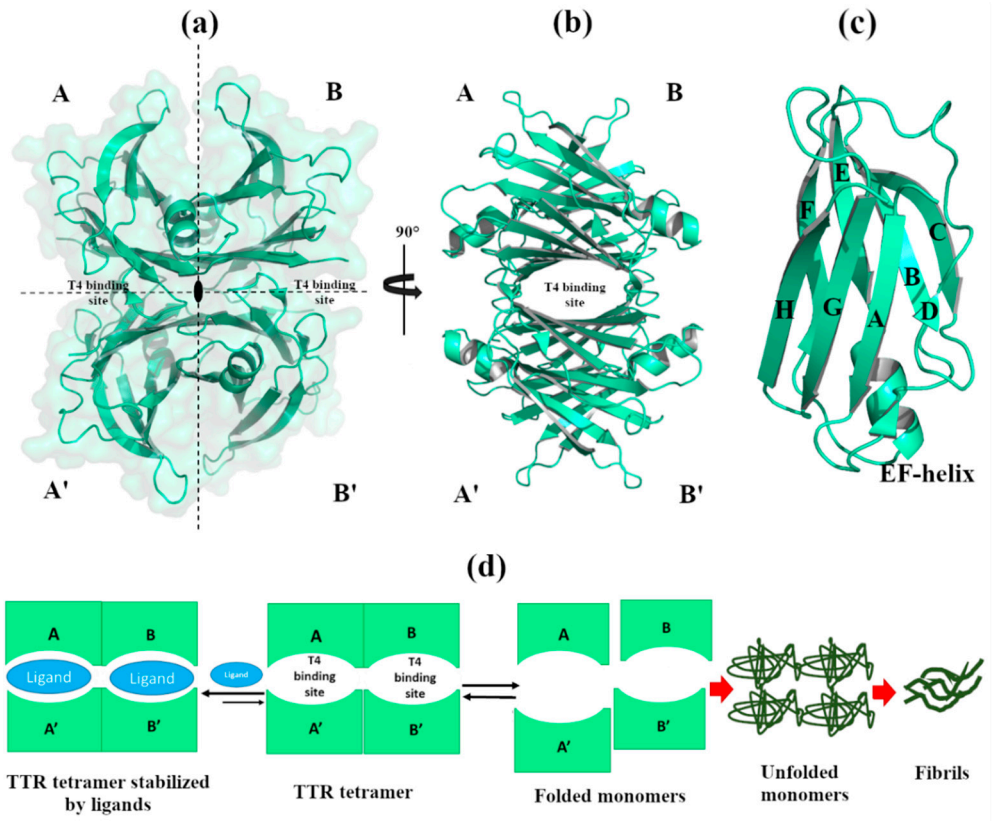

Figure 1. Graphical representation of the human transthyretin (TTR) crystal structure. The figure was created by author using the Protein Data Bank (PDB) id 4TQI [4]). (**a**) The TTR tetramer is composed by monomers A, A′, B, B′ assembled together around the 222-fold axis. The molecular surface is colored in pale green. (**b**) TTR tetramer, rotated of 90°, displays the T4 binding sites that cross the entire tetramer. (**c**) Structural details of monomer A. (**d**) Schematic representation of amyloidogenic pathway.

Studies report that in CSF, TTR is one of the principal proteins interacting with amyloid-β (Aβ) peptides. Much evidence supports the hypothesis that TTR prevents the formation of Aβ deposits and protects against neurodegeneration, although the exact mechanism remains unknown [5–7].

Under pathological conditions, wild-type TTR (wt-TTR) dissociates into partially unfolded monomers that can aggregate and form fibrils [8]. In fact, the high level of β-sheet secondary structure, exposed after tetramer dissociation, contributes to the intrinsic amyloidosis potential of the TTR protein. The aggregation of wt-TTR is related to senile systemic amyloidosis (SSA), where high levels of wt-TTR amyloid deposits in the heart, affecting about 25% of the world population over eighty-years of age [9]. More than a hundred point-mutations of TTR have been characterized (http://amyloidosismutations.com, accessed on 29 March 2021), and most of them induce the protein misfolding that favors TTR amyloidosis onset [10]. TTR variants are often associated with familial amyloid polyneuropathy (FAP), familial amyloid cardiomyopathy (FAC), and central nervous system amyloidosis (CNSA), where amyloid deposits are principally located in the peripheral nerves, heart, and central nervous system, respectively [11–13].

The exact molecular mechanism by which TTR undergoes a tetramer dissociation and forms amyloid fibrils in human has not yet been explained. It has been reported that, under physiological pH, a subunit exchange between an amyloidogenic tetramer (e.g., V30M TTR, associated to FAP) as well as a less amyloidogenic tetramer (wt-TTR) occurred, thus hypothesizing that the amyloidosis triggers once the subunit exchange happens [14]. Another hypothesis affirms that the dissociation of the TTR tetramer into monomers is the rate-limiting step for amyloid fibril formation [15].

The main hypothesis is that, during the fibril formation process, folded TTR monomers, wt and/or variant, undergo partial denaturation that has as a consequence, a reduced chance to reconstitute the native tetrameric structure [14,16–18], Figure 1d.

Among several therapeutic approaches against TTR amyloidosis, the stabilization of the tetramer seems to be a promising strategy [19]. In particular, the binding of natural and synthetic small molecules into the T4 binding sites, which are predominantly empty when circulate in plasma, stabilizes the native TTR tetramer, thus avoiding the evolution towards amyloidogenesis, Figure 1d [20–22].

Metal ions have been reported to play a relevant role in several amyloid-forming proteins. An in-vitro study conducted on Aβ peptides, reported that high concentrations of metals such as Zn^{2+}, Cu^{2+} and Fe^{2+} promote its aggregation [23]. Post-mortem investigation of Aβ plaques in AD patients shows higher accumulations of Cu, Fe and Zn ions compared to the normal levels detected in healthy brains [24]. The controversial assumption that abnormal concentrations of certain metals may lead to pathological events due to misaccumulation and irregular reactivity in AD, as well as in other neurodegenerative diseases, is still debated [25–27].

Concerning TTR, Wilkinson-White and Simon B. Easterbrook-Smith were the first to investigate, through in-vitro analyses, the effects of physiological metals Cu^{2+}, Zn^{2+}, Al^{3+}, and Fe^{3+} on amyloid formation of both wt-TTR and its mutants. In particular, V30M, L55P and T119M, which are the most common, the most aggressive, and the non-amyloidogenic variant, respectively. They show that, while Cu^{2+} and Zn^{2+} metal ions bind to both wt-TTR and its mutants, the corresponding effect on the rate of fibrillization is different, with the TTR variants more sensitive to metal binding [28].

Since then, several studies have appeared in the literature, focusing on the controversial role of metals in TTR structure and function. Here, we review the most important studies conducted on TTR in the presence of metals, and in particular, we highlight those concerning TTR conformational investigations. We group all conformational changes that have, until now, been observed in TTR structures when TTR binds metals. We also initiate discussions on the possible impact that metals can have on protein misfolding or neuroprotective function.

2. Effect of Metals in TTR Structure and Function

2.1. Non-Physiological Metals: Cr^{3+} and Re^{2+}

Starting from a previous study where two halides, iodine and chloride, were investigated for their ability to increase the stability of the TTR tetramer [29], T. Sato et al. screened several metal ions (Cu^{2+}, Zn^{2+}, Ca^{2+}, Co^{2+}, Cd^{2+}, Mn^{2+}, Fe^{3+} and Cr^{3+}) in order to evaluate their effect on TTR. Among these, only Cr^{3+} showed a significant reduction in amyloid fibril formation, favoring T4 binding with the tetramer, and stabilizing both wt-TTR and the V30M-TTR variant [30]. The stability of the tetramer was confirmed by calorimetric analyses performed at physiological and acid pH (25 μM TTR samples against 500 μM Cr^{3+}). The X-ray structure of wt-TTR in complex with Cr^{3+} was solved at 1.8 Å, and the anomalous difference Fourier maps displayed major peaks close to Glu54 (data not deposited) [30]. The authors suggested that Cr^{3+} can electrostatically neutralize this zone, pushing the T4 to bind TTR [30].

Crystal structures of wt-TTR, in complex with rhenium, were obtained by soaking TTR crystals in cryoprotectant solutions rich in tris-carbonyl derivatives, following a strategy already reported in the literature [31,32]. The initial purpose of this investigation was to study and try to solve the phase problem during the single-wavelength anomalous diffraction (SAD) experiments. Briefly, crystals were obtained by sitting-drop vapor-diffusion method from a reservoir solution of 21% polyethylene glycol 4000 (PEG4K), 0.14 M imidazole malate, pH 6.0 (PDB id:5K1J) as well as from 21% PEG4K, 0.14 M imidazole malate, pH 6.0, 3.6% polyethylene glycol monomethylether (MPEG5K), and 30 mM sodium acetate, pH 5.5 (PDB id 5K1N). For data collection, the first crystal was cryoprotected by soaking for 10 min into cryoprotectant solution composed of 40% of SM2 (12.5% ethylene glycol,

12.5% glycerol, 12.5% 1,2-propanediol, 25% DMSO and 37.5% 1,4-dioxane), 25% PEG 8K and 0.2 mM of rhenium derivative (PDB id:5K1J). The second one was cryoprotected with a solution of 40% SM3 (25% diethylene glycol, 25% ethylene glycol, 25% glycerol, 25% 1,4-dioxane), 25% PEG 8K and 0.5 mM of rhenium compound [31] (PDB id 5K1N). Interestingly, crystals soaked with a low concentration of rhenium derivatives gave structures that diffracted to 1.7 Å resolution, showing a new wt-TTR conformation. Both structures show a Re atom that coordinates with His88 in monomer B and B', Figure 2a.

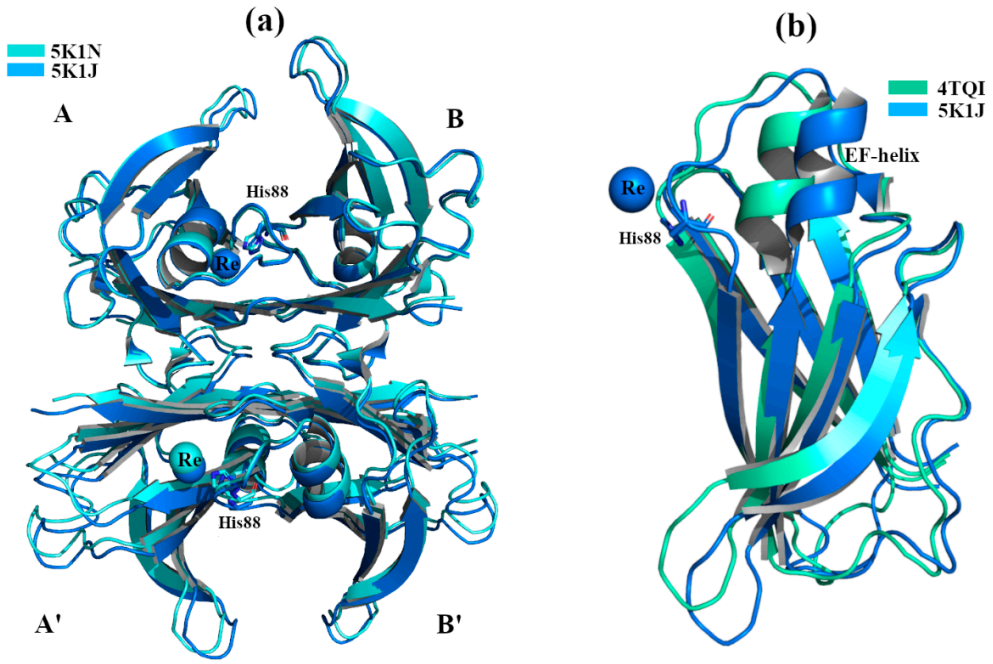

Figure 2. TTR crystal structures in complex with Re^{2+}. The figure was created by author downloading the appropriate PDB codes. (**a**) Superposition between the two crystals structures soaked with Re^{2+} under acidic conditions. The common Re^{2+} binding site is shown. (**b**) Superposition of monomers B between the standard conformation (PDB 4TQI) versus the new one (5K1J). The major difference is visible around the EF-helix of PDB structure 5K1J that is shifted.

The structural analysis highlighted that the tetramer is well conserved even if the monomers B and B' in the segment comprised of residues 72-94 (residues 72-90 correspond to EF-helix) are shifted, opening the thyroxin binding site B-B' while shrinking A-A' site, Figure 2a,b. This TTR conformation has never been observed before, even if its effect in the central channel is attributable to the well-known negative cooperativity of TTR [33].

Another region of TTR, usually characterized by considerable structural variations, is located between residues 94 to 104 (FG loop). The highest root mean square deviation value calculated on C-α (r.m.s.d.) is that calculated between the new structures and TTR the $P3_1$ polymorph (r.m.s.d. 2.74 Å) [31,34]. For more detailed information regarding the structural differences between the TTR-Re crystal complexes and other structures, we refer the reader to the original manuscript [31]. It has been hypothesized that this conformation obtained in the presence of Re, where the EF-helix swings away from the T4 binding site opening the dimer B-B', may represent the tetramer conformation that is able to interact with the Aβ peptide. This consideration is strengthened by previous studies, where it has been observed that Leu82 (EF-helix) and Leu110 (strand G) are key residues for the interaction between TTR and Aβ [35,36].

2.2. Physiological Metals

2.2.1. Zn^{2+}

Several studies report that Zn^{2+} binds to TTR, both in vitro and in vivo [28,37,38]. High levels of Zn^{2+} and Cu^{2+} ions induce the formation of TTR amyloid deposits in vitro, while chelating agents favor their disruption. In ex-vivo ocular amyloid deposits, from FAP patients with the V30M mutation, elevated concentrations of Zn^{2+} was found [37]. Starting from this evidence, it was hypothesized that Zn^{2+}, binding with TTR, might induce structural changes triggering its amyloidogenesis process.

X-ray crystal structure analyses of four engineered monomer TTRs (M-TTR, F87M/L110M) [39], in complex with Zn^{2+} at several concentrations, and at different pHs (pH 7.5, 6.5, 5.5, 4.6), revealed three possible Zn^{2+} binding sites (ZBS) [40]. Crystals were grown by hanging-drop vapour-diffusion method in a solution composed of 100 mM sodium citrate, 2.0 ammonium sulphate and 200 mM of zinc acetate. The C-α r.m.s.d. among the structures (PDB id: 3DGD, 3GPS, 3GRB, 3GRG) is less than 0.4 Å, indicating that they are very similar to each other, Figure 3a. The binding of Zn^{2+} with ZBS1 involves the two amino acids Cys10 and His56 and it does not lead to any significant conformational change. This suggests that the allocation of Zn^{2+} in ZBS1 is physiological and may prevent amyloidogenic character, Figure 3b [40].

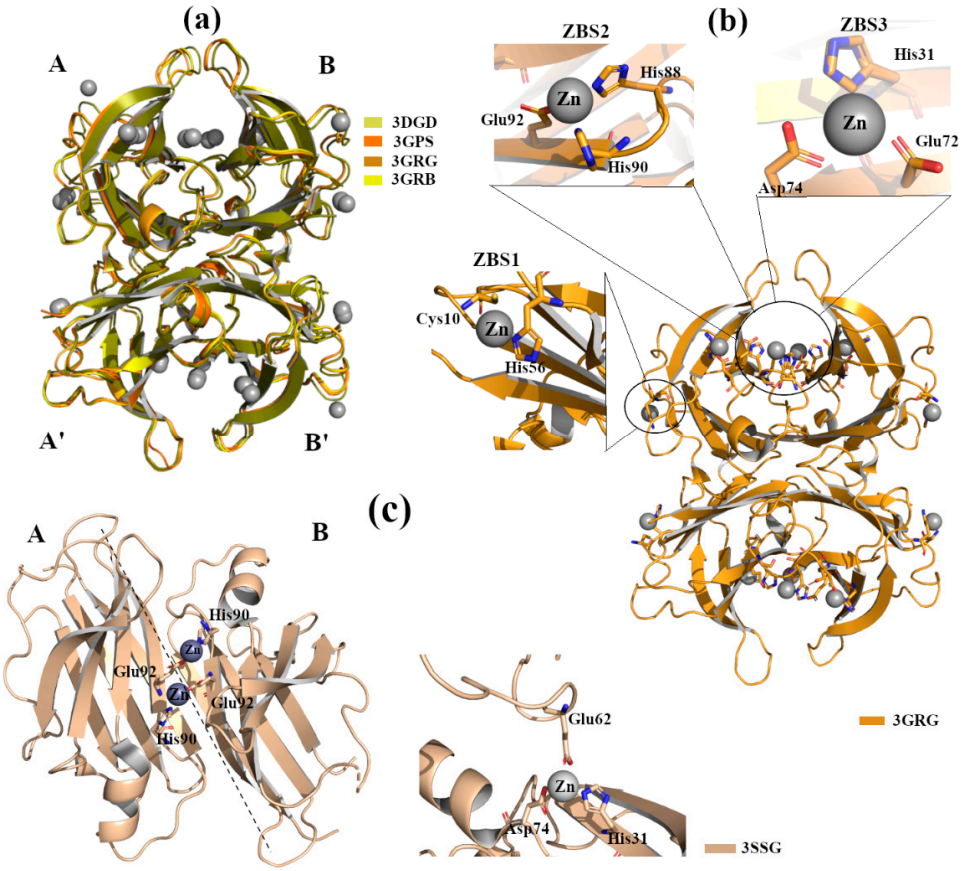

Figure 3. TTR crystal structures in complex with Zn^{2+}. The figure was created by author downloading the appropriate PDB codes. (**a**) Superposition of the four Zn^{2+}-M-TTR obtained at different pHs (PDB id: 3GRG pH 7.5, 3GRB pH 6.5, 3GPS pH 5.5, 3DGD pH 4.6). Zinc ions are colored in grey. (**b**) Graphical representation of ZBS1-3 in the M-TTR crystal structure (PDB id: 3GRG). (**c**) Graphical representation of ZBS1-2 in the L55P-TTR crystal structure (PDB id: 3SSG).

Moreover, the occupation of ZBS1 does not produce any effect on TTR-RBP interaction (the residues of TTR involved in the binding with RBP are Arg21, Val20, Leu82 and Ile-84) [41]. In contrast, in the presence of a higher Zn^{2+} concentration, the binding of Zn^{2+} to

ZBS2 (Hys88, Hys90 and Glu92) and ZBS3 (Glu72, Asp74 and Hys31) Figure 3b induces slight structural rearrangements around the α-helix at all tested pH. These modifications are comparable with those detected in other TTR structures crystallized without metals but at acidic pH [42]. Contrary to the effect observed for ZBS1, the involvement of ZBS2 and ZBS3 and their corresponding conformational changes affect the interaction of TTR with RBP [40].

TTR L55P is considered as one of the most aggressive amyloidogenic variants that accelerate pathology onset. Structural studies report that apo-TTR L55P, as well as TTR L55P in complex with 2,4-dinitrolphenol (DNP), possess the typical tetrameric structure. The only detected change is local in the monomers, where, due to a disorder of the short edge strand D, an extended loop between strands C and E appears [43,44].

The crystal structure of TTR L55P (PDB id: 3SSG), in complex with Zn^{2+}, does not show significant differences compared to apo-TTR, TTR L55P-DNP and the M-TTR-Zn^{2+} [45]. TTR L55P, in complex with Zn^{2+}, was grown by hanging-drop vapour-diffusion in presence of 3% w/v PEG 8000, 0.1M cacodylate pH 6.5, 5 mM Zn acetate. This X-ray structure shows two ZBS: ZBS1 is at an intra-dimer site that involves His90 from one monomer and Glu92 from the vicinal monomer, whilst ZBS2 is intra-tetramer, located between His31 and Asp74 from one monomer and Glu62 from symmetric monomer, Figure 3c. No Zn^{2+} ions are detected around Cys10 and/or His56; this might be related to the proximity of the point mutation L55P. Even if TTR L55P-Zn^{2+} does not show relevant conformational changes, it is interesting to highlight that Zn^{2+} binding induces a different tetragonal packing (space group $P4_22_12$) in the quaternary structure that could represent an ordered intermediate before evolving into an amyloidogenic conformation.

Recently, studies report that TTR can also be considered as an inducible metallopeptidase [38,46]. The TTR catalytic triad is composed of residues His88, His90 and Glu92, and its activation is modulated by bivalent metal ions. It has been demonstrated that, when TTR proteolytic activity is inhibited in vitro by metal chelators, Zn^{2+} and Mn^{2+} reestablished their full proteolytic activity, whereas other metals such as Fe^{2+} and Co^{2+} only partially reactivated the enzyme. This TTR proteolytic activity agrees with the hypotheses in which TTR behaves as a protease in neurodegenerative diseases such as AD and atherosclerosis. In fact, apoA-I and Aß can be cleaved by TTR, which might affect the onset of atherosclerosis and AD, respectively [47,48].

Despite several studies focusing on understanding whether the interaction between TTR and Zn^{2+} has a physiological or pathological role, the hypothesis is still debated.

2.2.2. Cu^{2+}, Fe^{2+} and Mn^{2+}

Biophysical studies employing light scattering and fluorescence spectroscopy demonstrate that Cu^{2+} binds to TTR; the presence of the metal induces some structural and functional effects on TTR [28]. Binding of Cu^{2+} provokes a dose-dependent decrease in Trp41 fluorescence intensity, suggesting a local perturbation around this zone. The same tendency was observed when Cu^{2+} binds TTR in the presence of 1-anilino-8-naphthalene sulfonate (ANS). ANS is a small fluorescent ligand able to bind both T4 binding sites and stabilize the TTR tetrameric structure [49,50]. The observation of a fluorescence perturbation upon Cu^{2+} binding suggests a local structural variation across the central channel [28]. Interestingly, the same study demonstrated that Cu^{2+} did not influence the rate of wt-TTR amyloid formation at pH 6.5 or 7.4. This trend was successively confirmed in a urea-induced dissociation experiment. Depending on the tested concentrations, Cu^{2+} did not show any effect on the tetramer dissociation, but, on the contrary, seemed to stabilize it. In contrast, in the L55P TTR mutant, Cu^{2+} favors tetramer dissociation and accelerates the process of amyloid formation [28].

As mentioned in the introduction, in contrast with its intrinsic amyloidogenic potential, TTR has a neuroprotective role in AD. TTR binds Aβ, participating in its clearance from the brain [6,51]. It has been hypothesized that metals might play a role in triggering this additional function of TTR.

Structural studies of TTR in complex with different metals confirm that Fe^{2+}, Cu^{2+} and Mn^{2+} bind to the protein, Figure 4a. TTR crystals were grown by sitting-drop vapor-diffusion, and the reservoir solution was filled with 21% of PEG4K, 0.14M imidazole malate, pH 6.0 or 21% of PEG4K, 0.14M imidazole malate, pH 6.0, 3.6% MPEG5K, and 30mM sodium acetate, pH 5.5. The cryoprotectant solution was composed of 40% of SM2 (12.5% ethylene glycol, 12.5% glycerol, 12.5% 1,2-propanediol, 25% DMSO and 37.5% 1,4-dioxane) 25% PEG 8K and 30mM of $CuCl_2$, $MnCl_2$ or $FeCl_2$. The X-ray crystal structure analysis of TTR in complex with Mn^{2+} did not show any significant structural differences. Two possible Mn^{2+} binding sites were detected around Asp99 and Glu66 in monomer A, and two, Glu66 and Asn98, in monomer B, Figure 4b [52]. In contrast, when wt-TTR crystals were treated with Cu^{2+}, these displayed a similar behavior of those soaked with Fe^{2+} (Figure 4a) and Re^{2+} [31,52]. The electron density map suggests that Cu^{2+} ions are located around His88, His90 and Asp74 for monomer B, and between His90 and Asp74 for monomer A, Figure 4c. A minor pick is detected close to Asp38, Figure 4c.

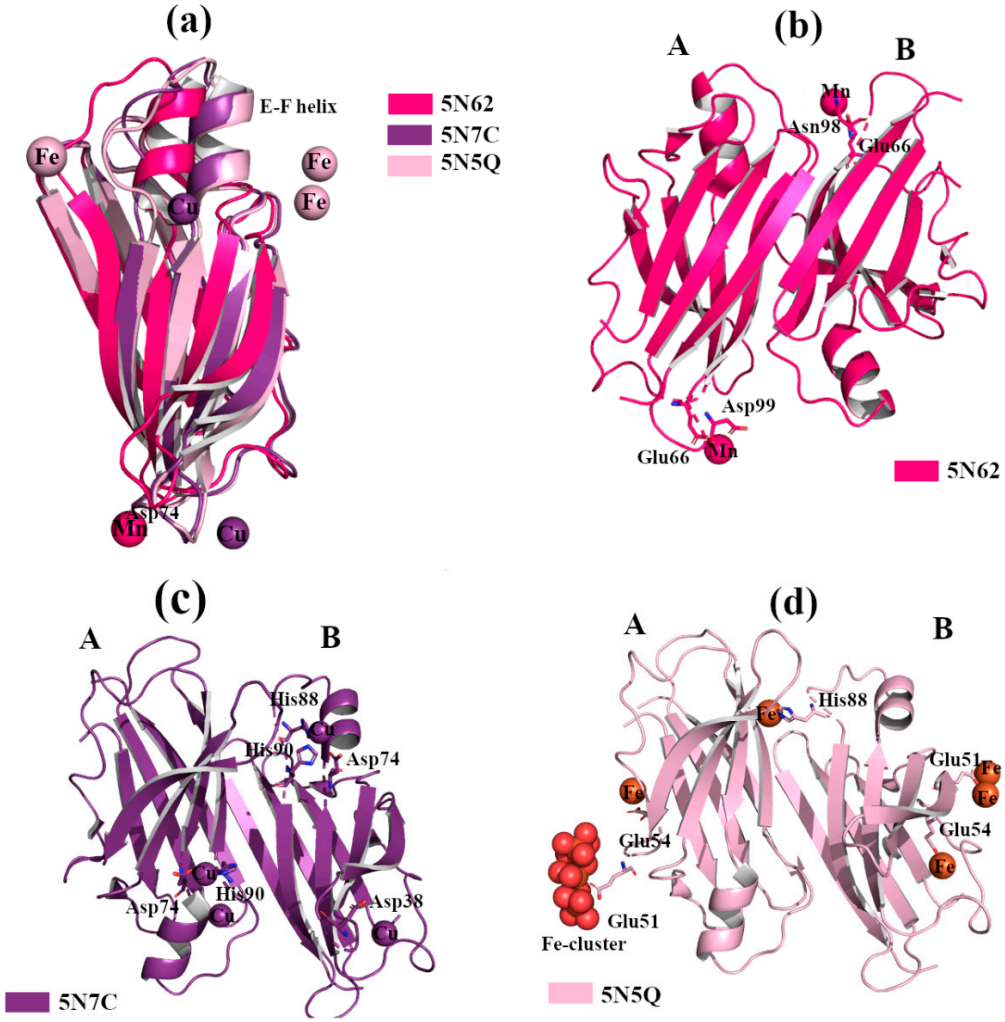

Figure 4. TTR crystal structures in complex with Mn^{2+}, Cu^{2+} and Fe^{2+}. The figure was created by author downloading the appropriate PDB codes. (**a**) Superposition of the B monomers of the three TTR crystal structures obtained in presence of Mn^{2+}, Cu^{2+} and Fe^{2+}, respectively (PDB id 5N62, 5N7C and 5N5Q). The EF-helix of TTR-Mn^{2+} crystal complex shows the classical conformation, while it is shifted for the other two metals complexes. (**b**) Graphical representation of the dimer A-B of TTR in complex with Mn^{2+}. (**c**) Graphical representation of the dimer A-B of TTR in complex with Cu^{2+}. (**d**) Graphical representation of dimer A-B of TTR in complex with Fe^{2+}.

Thus, Fe^{2+} and Cu^{2+}, but not Mn^{2+}, induce a conformational change in the wt-TTR tetramer, comparable to that observed in TTR-Re^{2+} crystal complex [52]. In order to verify if trivalent metals ions also induce conformational changes, several wt-TTR crystals were soaked with Al^{3+}, Gd^{3+} and Fe^{3+} following the same protocol. No structural modifications were found.

The binding of Fe^{2+} with TTR protein was confirmed via the strong anomalous signal registered in the phased anomalous difference Fourier map [53,54]. The highest peak is registered close to Glu51, a second site is located near Glu54 at the entrance of the T4 binding site, and another peak is detected around His88, Figure 4d. As previously seen in the rhenium-TTR structure, the conformational change affects only the β-strands E and F, and the short α-helix connecting them located in monomers B and B′ [52].

Interestingly, the conformational change, induced by Cu^{2+} and Fe^{2+}, modifies the dimer-dimer interface involving the TTR amino acid sequence, which is implicated in the interaction with Aβ peptides [35,55]. It is known that in the brains of AD patients, the concentration of metals (in particular Cu, Fe and Zn) is altered, and the amount of Cu^{2+} in Aβ plaque can reach 400 μM [24]. A bio-layer interferometry (BLI) study in solution revealed that a binding affinity between TTR and Aβ1-28 peptide is in nanomolar range when in the presence of Cu^{2+}, thus hinting that the TTR conformational change induced by Cu^{2+} and Fe^{2+} might be associated with TTR's ability to neutralize Aβ [52]. This experimental evidence suggests that the conformational change induced by Cu^{2+} and Fe^{2+} is not a structural artefact due to the soaking technique, but is probably related to the neuroprotective role that TTR possesses in the brain. This new conformation of TTR has inspired the design of PROteolysis-Targeting Chimeras (PROTAC) compounds that can induce the "active TTR conformation" favoring both the stabilization of TTR tetramer and the Aβ scavenger [56].

2.2.3. Ca^{2+}

The calcium ion, Ca^{2+}, is one of the most important metals involved in the regulation of cellular signalling pathways and tissue homeostasis. Several studies report that the dysregulation of Ca^{2+} is a key factor in the triggering of neurodegenerative processes [57]. TTR binds Ca^{2+} [58], and X-ray studies do not show any relevant structural changes in the wt-TTR tetrameric structure. TTR-Ca^{2+} crystal complexes were obtained by sitting drop vapour-diffusion from a solution containing 100mM HEPES, 200 mM $CaCl_2$, 28% PEG400, pH 7.5 (PDB id: 4MRB, 200 mM Ca^{2+} [59]) and 34–40% PEG 400, 400 mM $CaCl_2$, 0.1 M HEPES, pH 7.5 (4N85, 400 mM Ca^{2+}) [60]. The superposition of the two structures reveals that there is a common Ca^{2+} site between Glu66 and Asp99 of monomer A, while a second site is detected around N-terminus portions in the crystal at higher Ca^{2+} concentrations, Figure 5a,b. Different variants of TTR have been solved alone or in complex with ligands, in the presence of Ca^{2+}, and in these cases no relevant structural differences were detected [59,61,62].

Recently, studies in solution show that Ca^{2+} does not modify the environment around tryptophan residues, confirming that it does not induce global structural changes [63]. Interestingly, in the presence of Ca^{2+}, the binding between TTR and ANS decreases, suggesting that the T4 binding sites are less accessible. Deeper analysis confirmed that the fluorescent emission spectra, recorded at 275 nm, did not display any significant structural modifications [63]. However, the same study confirms that Ca^{2+} increases the rate of fibril formation in the TTR fibril formation assay. This suggests that the dysregulation of Ca^{2+} ions might have a role in the onset of TTR amyloidosis.

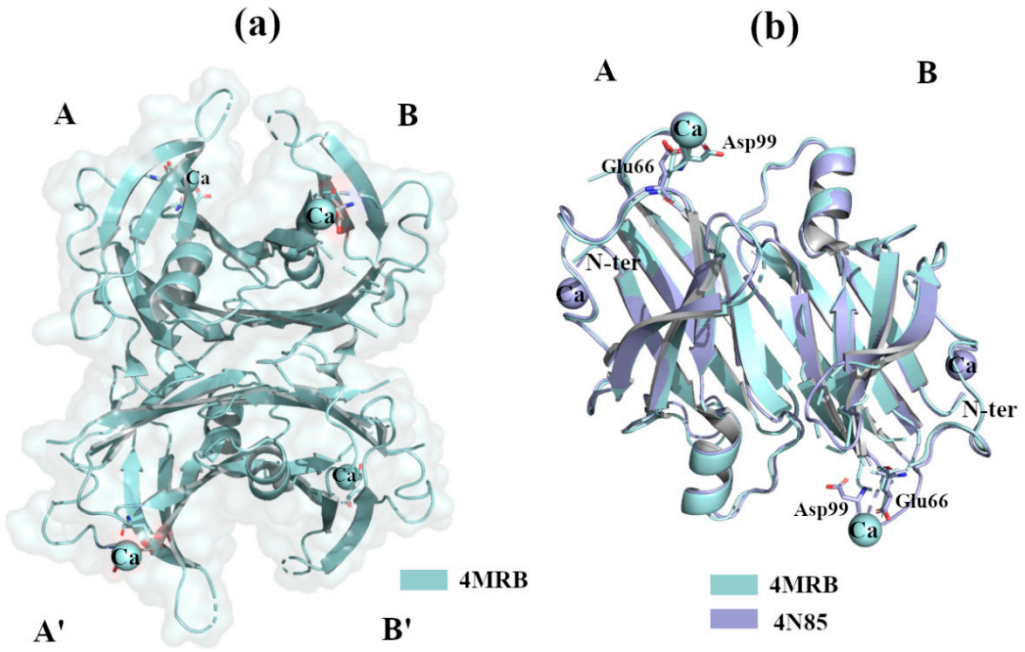

Figure 5. TTR crystal structures in complex with Ca^{2+}. The figure was created by author downloading the appropriate PDB codes. (**a**) Tetramer representation of TTR in complex with Ca^{2+}. (**b**) Superposition of the two dimers A-B of TTR in complex with Ca^{2+}.

3. Conclusions and Perspective

Metal ions have been found in several amyloid deposits, such as Aß plaques in AD, and α-synuclein plaques in Parkinson's diseases (PD) [23,64,65]. This evidence leads to the hypothesis that metal ions could be involved in the amyloidogenic process. Being an amyloid protein, many studies have been conducted on TTR to investigate if metal ions might have an important role in its amyloidogenic onset, or, if they may contribute to its stability and physiological role. Structural investigations, conducted via X-ray crystallography of TTR in the presence of different metal ions, has emerged in the last few years as a useful tool to explore the possible conformational changes in the wild-type and/or mutants. A direct comparison of the solved crystal structures provides insights into the physiological or pathological role of TTR.

The potential role of Zn^{2+} remains under debate; on the one hand, Zn^{2+} prevents conformational changes upon binding to ZBS1, and it behaves as a cofactor for the physiological activity of TTR. On the other hand, its involvement in the ZBS2 and ZBS3 suggests a possible rearrangement of the EF-helix, which could affect its retinol transport activity. The proteolytic activity of TTR is restored in the presence of Zn^{2+}, but at the same time, Zn^{2+} has been proved to induce a different tetragonal packing in the quaternary structure, which could be involved in its amyloidogenic process. More efforts should be employed in order to better explain under which conditions Zn^{2+} acts as a protective element that stabilizes the correct folding of the protein, and when it instead becomes pathological.

Structural studies of TTR in complex with different metals confirm that Fe^{2+}, Cu^{2+} and Mn^{2+} are able to bind the protein. While Mn^{2+} does not to have an important impact on the global structure, Fe^{2+} and Cu^{2+} modify the dimer–dimer interface involving the TTR peptide sequence, which was shown to be implicated in the interaction with the Aβ peptide. This modification was also shown to be comparable to that observed in TTR-Re^{2+} crystal complex, and to affect the EF-helix sequence. This observation suggests the hypothesis that metal-bivalent ions, especially Cu^{2+}, are important cofactors of the TTR protein–protein interaction pattern that is physiologically important for neuroprotection.

Finally, one of the physiological metals that could be more involved in the amyloidogenic process of TTR is Ca^{2+}. A dysregulation of Ca^{2+} homeostasis would seem to affect the propensity of TTR to form fibrils.

In conclusion, this general overview highlights that most of the main conformational changes observed in TTR crystals, soaked in the presence of physiological metal ions, seem to occur in the proximity of an EF-helix, or at least affect its stability and positioning. This consideration allows us to hypothesize the interesting role of the helix as a possible "hot spot" sequence of either the proteolytic activity, or the protein-protein interaction pattern of TTR, which are both mediated by metal ions. This behavior mediates the neuro-protection role of TTR in neurodegeneration or atherosclerosis. Conversely, when the metal ions do not show any significant structural differences, they often affect the physiological transport activity of TTR, or influence its amyloidogenic character.

This review represents a general consideration for future development of new molecules which might behave either as scavenger, or as metal chelators, and whose goal is to enhance the physiologically positive role that TTR has when its tetramer structure remains stable.

Author Contributions: L.C. and N.T. writing—original draft preparation, L.C. made all figures, W.S., S.N., and E.O. review and editing. All authors have read and agreed to the published version of the manuscript.

Funding: This research was funded by the Italian Ministero dell'Istruzione, dell'Universitá e della Ricerca (PRIN 2017SNRXH3).

Data Availability Statement: Data Availability Statements in section "MDPI Research Data Policies" at https://www.mdpi.com/ethics (accessed on 29 March 2021).

Conflicts of Interest: The authors declare no conflict of interest.

References

1. Aldred, A.R.; Brack, C.M.; Schreiber, G. The Cerebral Expression of Plasma Protein Genes in Different Species. *Comp. Biochem. Physiol. Part B Biochem. Mol. Biol.* **1995**, *111*, 1–15. [CrossRef]
2. Hamilton, J.A.; Benson, M.D. Transthyretin: A Review from a Structural Perspective. *Cell. Mol. Life Sci. CMLS* **2001**, *58*, 1491–1521. [CrossRef]
3. Wojtczak, A.; Neumann, P.; Cody, V. Structure of a New Polymorphic Monoclinic Form of Human Transthyretin at 3 Å Resolution Reveals a Mixed Complex between Unliganded and T4-Bound Tetramers of TTR. *Acta Crystallogr. Sect. D Biol. Crystallogr.* **2001**, *57*, 957–967. [CrossRef]
4. Ciccone, L.; Nencetti, S.; Rossello, A.; Tepshi, L.; Stura, E.A.; Orlandini, E. X-ray Crystal Structure and Activity of Fluorenyl-Based Compounds as Transthyretin Fibrillogenesis Inhibitors. *J. Enzym. Inhib. Med. Chem.* **2016**, *31*, 824–833. [CrossRef] [PubMed]
5. Costa, R.; Gonçalves, A.; Saraiva, M.J.; Cardoso, I. Transthyretin Binding to A-Beta Peptide—Impact on A-Beta Fibrillogenesis and Toxicity. *FEBS Lett.* **2008**, *582*, 936–942. [CrossRef]
6. Alemi, M.; Gaiteiro, C.; Ribeiro, C.A.; Santos, L.M.; Gomes, J.R.; Oliveira, S.M.; Couraud, P.-O.; Weksler, B.; Romero, I.; Saraiva, M.J.; et al. Transthyretin Participates in Beta-Amyloid Transport from the Brain to the Liver- Involvement of the Low-Density Lipoprotein Receptor-Related Protein 1? *Sci. Rep.* **2016**, *6*, 1–15. [CrossRef]
7. Ciccone, L.; Shi, C.; di Lorenzo, D.; Van Baelen, A.-C.; Tonali, N. The Positive Side of the Alzheimer's Disease Amyloid Cross-Interactions: The Case of the Aβ 1-42 Peptide with Tau, TTR, CysC, and ApoA1. *Molecules* **2020**, *25*, 2439. [CrossRef]
8. Lashuel, H.A.; Lai, Z.; Kelly, J.W. Characterization of the Transthyretin Acid Denaturation Pathways by Analytical Ultracentrifugation: Implications for Wild-Type, V30M, and L55P Amyloid Fibril Formation. *Biochemistry* **1998**, *37*, 17851–17864. [CrossRef] [PubMed]
9. Cornwell, G.G.; Murdoch, W.L.; Kyle, R.A.; Westermark, P.; Pitkänen, P. Frequency and Distribution of Senile Cardiovascular Amyloid: A Clinicopathologic Correlation. *Am. J. Med.* **1983**, *75*, 618–623. [CrossRef]
10. Connors, L.H.; Lim, A.; Prokaeva, T.; Roskens, V.A.; Costello, C.E. Tabulation of Human Transthyretin (TTR) Variants, 2003. *Amyloid* **2003**, *10*, 160–184. [CrossRef]
11. Saraiva, M.J.; Birken, S.; Costa, P.P.; Goodman, D.S. Amyloid Fibril Protein in Familial Amyloidotic Polyneuropathy, Portuguese Type. Definition of Molecular Abnormality in Transthyretin (Prealbumin). *J. Clin. Investig.* **1984**, *74*, 104–119. [CrossRef]
12. Westermark, P.; Sletten, K.; Johansson, B.; Cornwell, G.G. Fibril in Senile Systemic Amyloidosis Is Derived from Normal Transthyretin. *Proc. Natl. Acad. Sci. USA* **1990**, *87*, 2843–2845. [CrossRef]
13. Benson, M.D. Leptomeningeal Amyloid and Variant Transthyretins. *Am. J. Pathol.* **1996**, *148*, 351–354.
14. Schneider, F.; Hammarström, P.; Kelly, J.W. Transthyretin Slowly Exchanges Subunits under Physiological Conditions: A Convenient Chromatographic Method to Study Subunit Exchange in Oligomeric Proteins. *Protein Sci.* **2001**, *10*, 1606–1613. [CrossRef]
15. Sousa, M.M.; Saraiva, M.J. Neurodegeneration in Familial Amyloid Polyneuropathy: From Pathology to Molecular Signaling. *Prog. Neurobiol.* **2003**, *71*, 385–400. [CrossRef]

16. Foss, T.R.; Wiseman, R.L.; Kelly, J.W. The Pathway by Which the Tetrameric Protein Transthyretin Dissociates. *Biochemistry* **2005**, *44*, 15525–15533. [CrossRef] [PubMed]
17. Yee, A.W.; Aldeghi, M.; Blakeley, M.P.; Ostermann, A.; Mas, P.J.; Moulin, M.; de Sanctis, D.; Bowler, M.W.; Mueller-Dieckmann, C.; Mitchell, E.P.; et al. A Molecular Mechanism for Transthyretin Amyloidogenesis. *Nat. Commun.* **2019**, *10*, 925. [CrossRef]
18. Colon, W.; Kelly, J.W. Partial Denaturation of Transthyretin Is Sufficient for Amyloid Fibril Formation in Vitro. *Biochemistry* **1992**, *31*, 8654–8660. [CrossRef]
19. Merlini, G.; Coelho, T.; Waddington Cruz, M.; Li, H.; Stewart, M.; Ebede, B. Evaluation of Mortality During Long-Term Treatment with Tafamidis for Transthyretin Amyloidosis with Polyneuropathy: Clinical Trial Results up to 8.5 Years. *Neurol. Ther.* **2020**, *9*, 105–115. [CrossRef] [PubMed]
20. Guo, X.; Liu, Z.; Zheng, Y.; Li, Y.; Li, L.; Liu, H.; Chen, Z.; Wu, L. Review on the Structures and Activities of Transthyretin Amyloidogenesis Inhibitors. *Drug Des. Dev. Ther.* **2020**, *14*, 1057–1081. [CrossRef] [PubMed]
21. Ciccone, L.; Tonali, N.; Nencetti, S.; Orlandini, E. Natural Compounds as Inhibitors of Transthyretin Amyloidosis and Neuroprotective Agents: Analysis of Structural Data for Future Drug Design. *J. Enzym. Inhib. Med. Chem.* **2020**, *35*, 1145–1162. [CrossRef] [PubMed]
22. Ortore, G.; Orlandini, E.; Braca, A.; Ciccone, L.; Rossello, A.; Martinelli, A.; Nencetti, S. Targeting Different Transthyretin Binding Sites with Unusual Natural Compounds. *ChemMedChem* **2016**, *11*, 1865–1874. [CrossRef]
23. Atwood, C.S.; Moir, R.D.; Huang, X.; Scarpa, R.C.; Bacarra, N.M.E.; Romano, D.M.; Hartshorn, M.A.; Tanzi, R.E.; Bush, A.I. Dramatic Aggregation of Alzheimer Aβ by Cu(II) Is Induced by Conditions Representing Physiological Acidosis. *J. Biol. Chem.* **1998**, *273*, 12817–12826. [CrossRef]
24. Lovell, M.A.; Robertson, J.D.; Teesdale, W.J.; Campbell, J.L.; Markesbery, W.R. Copper, Iron and Zinc in Alzheimer's Disease Senile Plaques. *J. Neurol. Sci.* **1998**, *158*, 47–52. [CrossRef]
25. Liu, Y.; Nguyen, M.; Robert, A.; Meunier, B. Metal Ions in Alzheimer's Disease: A Key Role or Not? *Acc. Chem. Res.* **2019**, *52*, 2026–2035. [CrossRef]
26. Bisaglia, M.; Bubacco, L. Copper Ions and Parkinson's Disease: Why Is Homeostasis So Relevant? *Biomolecules* **2020**, *10*, 195. [CrossRef] [PubMed]
27. Dales, J.-P.; Desplat-Jégo, S. Metal Imbalance in Neurodegenerative Diseases with a Specific Concern to the Brain of Multiple Sclerosis Patients. *Int. J. Mol. Sci.* **2020**, *21*, 9105. [CrossRef] [PubMed]
28. Wilkinson-White, L.E.; Easterbrook-Smith, S.B. Characterization of the Binding of Cu(II) and Zn(II) to Transthyretin: Effects on Amyloid Formation. *Biochemistry* **2007**, *46*, 9123–9132. [CrossRef]
29. Hörnberg, A.; Hultdin, U.W.; Olofsson, A.; Sauer-Eriksson, A.E. The Effect of Iodide and Chloride on Transthyretin Structure and Stability. *Biochemistry* **2005**, *44*, 9290–9299. [CrossRef]
30. Sato, T.; Ando, Y.; Susuki, S.; Mikami, F.; Ikemizu, S.; Nakamura, M.; Suhr, O.; Anraku, M.; Kai, T.; Suico, M.A.; et al. Chromium(III) Ion and Thyroxine Cooperate to Stabilize the Transthyretin Tetramer and Suppress in Vitro Amyloid Fibril Formation. *FEBS Lett.* **2006**, *580*, 491–496. [CrossRef]
31. Ciccone, L.; Policar, C.; Stura, E.A.; Shepard, W. Human TTR Conformation Altered by Rhenium Tris-Carbonyl Derivatives. *J. Struct. Biol.* **2016**, *195*, 353–364. [CrossRef]
32. Ciccone, L.; Vera, L.; Tepshi, L.; Rosalia, L.; Rossello, A.; Stura, E.A. Multicomponent Mixtures for Cryoprotection and Ligand Solubilization. *Biotechnol. Rep.* **2015**, *7*, 120–127. [CrossRef] [PubMed]
33. Neumann, P.; Cody, V.; Wojtczak, A. Structural Basis of Negative Cooperativity in Transthyretin. *Acta Biochim. Pol.* **2001**, *48*, 867–875. [CrossRef]
34. Polsinelli, I.; Nencetti, S.; Shepard, W.; Ciccone, L.; Orlandini, E.; Stura, E.A. A New Crystal Form of Human Transthyretin Obtained with a Curcumin Derived Ligand. *J. Struct. Biol.* **2016**, *194*, 8–17. [CrossRef] [PubMed]
35. Du, J.; Cho, P.Y.; Yang, D.T.; Murphy, R.M. Identification of Beta-Amyloid-Binding Sites on Transthyretin. *Protein Eng. Des. Sel.* **2012**, *25*, 337–345. [CrossRef] [PubMed]
36. Yang, D.T.; Joshi, G.; Cho, P.Y.; Johnson, J.A.; Murphy, R.M. Transthyretin as Both a Sensor and a Scavenger of β-Amyloid Oligomers. *Biochemistry* **2013**, *52*, 2849–2861. [CrossRef] [PubMed]
37. Susuki, S.; Ando, Y.; Sato, T.; Nishiyama, M.; Miyata, M.; Suico, M.A.; Shuto, T.; Kai, H. Multi-Elemental Analysis of Serum and Amyloid Fibrils in Familial Amyloid Polyneuropathy Patients. *Amyloid* **2008**, *15*, 108–116. [CrossRef]
38. Liz, M.A.; Leite, S.C.; Juliano, L.; Saraiva, M.J.; Damas, A.M.; Bur, D.; Sousa, M.M. Transthyretin Is a Metallopeptidase with an Inducible Active Site. *Biochem. J.* **2012**, *443*, 769–778. [CrossRef]
39. Jiang, X.; Smith, C.S.; Petrassi, H.M.; Hammarström, P.; White, J.T.; Sacchettini, J.C.; Kelly, J.W. An Engineered Transthyretin Monomer That Is Nonamyloidogenic, Unless It Is Partially Denatured. *Biochemistry* **2001**, *40*, 11442–11452. [CrossRef]
40. Palmieri, L.d.C.; Lima, L.M.T.R.; Freire, J.B.B.; Bleicher, L.; Polikarpov, I.; Almeida, F.C.L.; Foguel, D. Novel Zn^{2+}-Binding Sites in Human Transthyretin: Implications for Amyloidogenesis and Retinol-Binding Protein Recognition. *J. Biol. Chem.* **2010**, *285*, 31731–31741. [CrossRef]
41. Naylor, H.M.; Newcomer, M.E. The Structure of Human Retinol-Binding Protein (RBP) with Its Carrier Protein Transthyretin Reveals an Interaction with the Carboxy Terminus of RBP. *Biochemistry* **1999**, *38*, 2647–2653. [CrossRef] [PubMed]
42. Palaninathan, S.K.; Mohamedmohaideen, N.N.; Snee, W.C.; Kelly, J.W.; Sacchettini, J.C. Structural Insight into PH-Induced Conformational Changes within the Native Human Transthyretin Tetramer. *J. Mol. Biol.* **2008**, *382*, 1157–1167. [CrossRef]

43. Morais-de-Sá, E.; Neto-Silva, R.M.; Pereira, P.J.; Saraiva, M.J.; Damas, A.M. The Binding of 2, 4-Dinitrophenol to Wild-Type and Amyloidogenic Transthyretin. *Acta Crystallogr. Sect. D Biol. Crystallogr.* **2006**, *62*, 512–519. [CrossRef] [PubMed]
44. Cendron, L.; Trovato, A.; Seno, F.; Folli, C.; Alfieri, B.; Zanotti, G.; Berni, R. Amyloidogenic Potential of Transthyretin Variants. *J. Biol. Chem.* **2009**, *284*, 25832–25841. [CrossRef] [PubMed]
45. Castro-Rodrigues, A.F.; Gales, L.; Saraiva, M.J.; Damas, A.M. Structural Insights into a Zinc-Dependent Pathway Leading to Leu55Pro Transthyretin Amyloid Fibrils. *Acta Crystallogr. D Biol. Crystallogr.* **2011**, *67*, 1035–1044. [CrossRef]
46. Gouvea, I.E.; Kondo, M.Y.; Assis, D.M.; Alves, F.M.; Liz, M.A.; Juliano, M.A.; Juliano, L. Studies on the Peptidase Activity of Transthyretin (TTR). *Biochimie* **2013**, *95*, 215–223. [CrossRef] [PubMed]
47. Costa, R.; Ferreira-da-Silva, F.; Saraiva, M.J.; Cardoso, I. Transthyretin Protects against A-Beta Peptide Toxicity by Proteolytic Cleavage of the Peptide: A Mechanism Sensitive to the Kunitz Protease Inhibitor. *PLoS ONE* **2008**, *3*, e2899. [CrossRef]
48. Liz, M.A.; Gomes, C.M.; Saraiva, M.J.; Sousa, M.M. ApoA-I Cleaved by Transthyretin Has Reduced Ability to Promote Cholesterol Efflux and Increased Amyloidogenicity. *J. Lipid Res.* **2007**, *48*, 2385–2395. [CrossRef]
49. Cheng, S.-Y.; Pages, R.A.; Saroff, H.A.; Edelhoch, H.; Robbins, J. Analysis of Thyroid Hormone Binding to Human Serum Prealbumin by 8-Anilinonaphthalene-1-Sulfonate Fluorescence. *Biochemistry* **1977**, *16*, 3707–3713. [CrossRef]
50. Lima, L.M.T.R.; Silva, V.d.A.; Palmieri, L.d.C.; Oliveira, M.C.B.R.; Foguel, D.; Polikarpov, I. Identification of a Novel Ligand Binding Motif in the Transthyretin Channel. *Bioorg. Med. Chem.* **2010**, *18*, 100–110. [CrossRef]
51. Li, X.; Zhang, X.; Ladiwala, A.R.A.; Du, D.; Yadav, J.K.; Tessier, P.M.; Wright, P.E.; Kelly, J.W.; Buxbaum, J.N. Mechanisms of Transthyretin Inhibition of -Amyloid Aggregation In Vitro. *J. Neurosci.* **2013**, *33*, 19423–19433. [CrossRef]
52. Ciccone, L.; Fruchart-Gaillard, C.; Mourier, G.; Savko, M.; Nencetti, S.; Orlandini, E.; Servent, D.; Stura, E.A.; Shepard, W. Copper Mediated Amyloid-β Binding to Transthyretin. *Sci. Rep.* **2018**, *8*, 13744. [CrossRef] [PubMed]
53. Evans, G.; Pettifer, R.F. CHOOCH: A Program for Deriving Anomalous-Scattering Factors from X-Ray Fluorescence Spectra. *J. Appl. Cryst.* **2001**, *34*, 82–86. [CrossRef]
54. Polsinelli, I.; Savko, M.; Rouanet-Mehouas, C.; Ciccone, L.; Nencetti, S.; Orlandini, E.; Stura, E.A.; Shepard, W. Comparison of Helical Scan and Standard Rotation Methods in Single-Crystal X-Ray Data Collection Strategies. *J. Synchrotron Radiat.* **2017**, *24*, 42–52. [CrossRef]
55. Du, J.; Murphy, R.M. Characterization of the Interaction of β-Amyloid with Transthyretin Monomers and Tetramers. *Biochemistry* **2010**, *49*, 8276–8289. [CrossRef] [PubMed]
56. Tonali, N.; Nencetti, S.; Orlandini, E.; Ciccone, L. Application of PROTAC Strategy to TTR-Aβ Protein-Protein Interaction for the Development of Alzheimer's Disease Drugs. *Neural Regen. Res.* **2021**, *16*, 1554. [CrossRef] [PubMed]
57. Alvarez, J.; Alvarez-Illera, P.; García-Casas, P.; Fonteriz, R.I.; Montero, M. The Role of Ca^{2+} Signaling in Aging and Neurodegeneration: Insights from Caenorhabditis Elegans Models. *Cells* **2020**, *9*, 204. [CrossRef]
58. Scott, B.J.; Bradwell, A.R. Identification of the Serum Binding Proteins for Iron, Zinc, Cadmium, Nickel, and Calcium. *Clin. Chem.* **1983**, *29*, 629–633. [CrossRef] [PubMed]
59. Mangione, P.P.; Porcari, R.; Gillmore, J.D.; Pucci, P.; Monti, M.; Porcari, M.; Giorgetti, S.; Marchese, L.; Raimondi, S.; Serpell, L.C.; et al. Proteolytic Cleavage of Ser52Pro Variant Transthyretin Triggers Its Amyloid Fibrillogenesis. *Proc. Natl. Acad. Sci. USA* **2014**, *111*, 1539–1544. [CrossRef]
60. Yokoyama, T.; Kosaka, Y.; Mizuguchi, M. Crystal Structures of Human Transthyretin Complexed with Glabridin. *J. Med. Chem.* **2014**, *57*, 1090–1096. [CrossRef]
61. Yokoyama, T.; Kosaka, Y.; Mizuguchi, M. Inhibitory Activities of Propolis and Its Promising Component, Caffeic Acid Phenethyl Ester, against Amyloidogenesis of Human Transthyretin. *J. Med. Chem.* **2014**, *57*, 8928–8935. [CrossRef] [PubMed]
62. Murakami, T.; Yokoyama, T.; Mizuguchi, M.; Toné, S.; Takaku, S.; Sango, K.; Nishimura, H.; Watabe, K.; Sunada, Y. A Low Amyloidogenic E61K Transthyretin Mutation May Cause Familial Amyloid Polyneuropathy. *J. Neurochem.* **2020**. [CrossRef]
63. Wieczorek, E.; Kędracka-Krok, S.; Bystranowska, D.; Ptak, M.; Wiak, K.; Wygralak, Z.; Jankowska, U.; Ożyhar, A. Destabilisation of the Structure of Transthyretin Is Driven by Ca^{2+}. *Int. J. Biol. Macromol.* **2021**, *166*, 409–423. [CrossRef] [PubMed]
64. Uversky, V.N.; Li, J.; Fink, A.L. Metal-Triggered Structural Transformations, Aggregation, and Fibrillation of Human α-Synuclein. *J. Biol. Chem.* **2001**, *276*, 44284–44296. [CrossRef] [PubMed]
65. Rasia, R.M.; Bertoncini, C.W.; Marsh, D.; Hoyer, W.; Cherny, D.; Zweckstetter, M.; Griesinger, C.; Jovin, T.M.; Fernandez, C.O. Structural Characterization of Copper(II) Binding to -Synuclein: Insights into the Bioinorganic Chemistry of Parkinson's Disease. *Proc. Natl. Acad. Sci. USA* **2005**, *102*, 4294–4299. [CrossRef] [PubMed]